

High-Power Squeeze-Type Phase Shifter at W-Band

Marc E. Hill, Richard S. Callin, Mike Seidel, and David H. Whittum

Abstract—We describe the design, fabrication, and bench study of a millimeter-wave phase shifter employed as a high-power recirculator for a traveling-wave resonator circuit. The oxygen-free electronic-grade copper phase shifter was prepared by electrodischarge machining. Measured phase-shifter characteristics are presented and compared with theory. The phase shifter was employed in a traveling-wave circuit at 91.4 GHz with a circulating power of 0.2 MW and subjected to fields greater than 10 MV/m without evidence of breakdown.

Index Terms—High-power phase shifters, millimeter-wave phase shifters, microwave phase shifters.

High-energy physics requires ever more compact charged particle accelerators, employing ultrahigh electric-field gradients, in excess of 100 MV/m. Recent experiments at *X*-band indicate that such fields are difficult to maintain due to breakdown, field emission, and damage from pulsed heating [1]. To surpass the 100-MV/m barrier, scalings for trapping and pulsed heating suggest that miniature accelerator structures, scaled up in frequency to *W*-band, may permit reliable operation [2]. To access the 100-MV/m range in the laboratory, the absence of a high-power *W*-band source has motivated tests on an accelerator beamline, in what is essentially a relativistic klystron configuration, as seen in Fig. 1(a). In such a configuration, with the 0.5-A 300-MeV *X*-band bunched beam available in our laboratory, it is possible to achieve 10-MV/m fields in a single *W*-band resonator [3]. However, to achieve another order of magnitude in the peak field, to reach the 100-MV/m level, we require either a long transfer structure, with attendant tight tolerances in fabrication and assembly, or a short structure, but with recirculation of power from the output to input. The choices are illustrated in Fig. 1. Recirculation in this fashion requires a phase shifter, as the power developed in the circuit depends on the phase length of the recirculator arm. Commercial components are not adequate for such work, where vacuum compatibility and high peak power are concerns. In this paper, we describe the design, fabrication, and bench test of a squeeze-type phase shifter suitable for the circuit of Fig. 1(b).

The squeeze-type shifter we envision is that pictured in Fig. 2, consisting of a length of WR10 waveguide, with standard WR10 inner and outer dimensions ($a = 0.10$ in, $b = 0.05$ in, and $A = 0.18$ in, $B = 0.13$ in outer) and single-mode propagation in the 59–118-GHz range.

The waveguide can be compressed in the wide (a) dimension to provide a phase shift. The actual waveguide will be bent to form a U shape; meanwhile, the phase length may be understood from the scaling for straight WR10. Changing the width of the waveguide changes the guide wavenumber β and, therefore, the phase length of the guide

$$\phi = \int_0^L \beta ds \quad (1)$$

$$\beta = \frac{2\pi}{\lambda} \sqrt{1 - \left(\frac{\lambda}{2a}\right)^2} \quad (2)$$

Manuscript received September 28, 2000. This work was supported by the U.S. Department of Energy under Contract DE-AC03-76SF00515.

M. E. Hill is with the Department of Physics, Harvard University, Cambridge, MA 02138 USA.

R. S. Callin and D. H. Whittum are with the Stanford Linear Accelerator Center, Stanford University, Stanford, CA 94309 USA.

M. Seidel is with Deutsches Elektronen Synchrotron (DESY), Hamburg 22607, Germany.

Publisher Item Identifier S 0018-9480(02)04045-0.

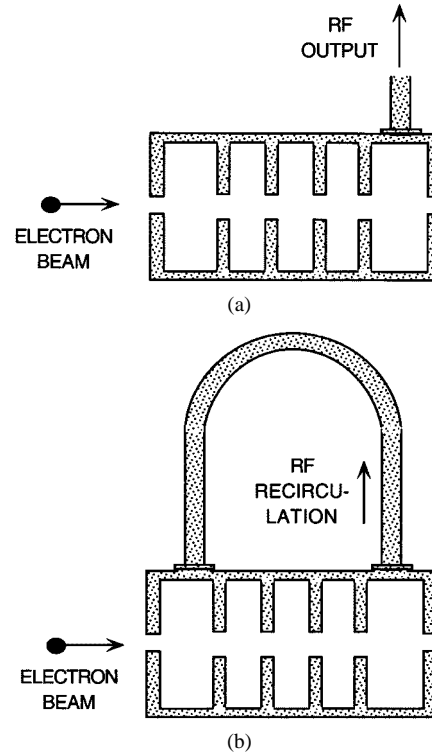


Fig. 1. Configurations for *W*-band power generation employing a multicavity accelerator. (a) In single-pass mode. (b) With recirculation of the millimeter-wave power. The drive electron beam consists of a train of bunches.

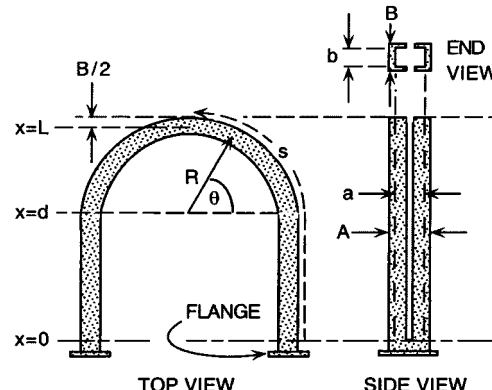


Fig. 2. Sketches of the squeeze-type phase shifter, not to scale, showing radius of curvature R , waveguide inner dimensions $a \times b$, and outer dimensions $A \times B$.

where a is the broad wall dimension and λ is the free-space wavelength at the desired frequency.

For small deviations δa in the waveguide width, the change in phase length is

$$\Delta\phi = \frac{\pi^2}{a^3 \beta} \int \delta a(s) ds \quad (3)$$

where s is the arc length around the phase shifter, as seen in Fig. 2. The variation δa is a function of distance from the cut x [4] as follows:

$$\delta a(x) = \frac{\Delta a}{2} \left[3 \left(\frac{x}{L} \right)^2 - \left(\frac{x}{L} \right)^3 \right] \quad (4)$$

where the end-point deviation is Δa . The geometry, coordinates, and dimensions are shown in Fig. 2. Integrating, we find the phase-length

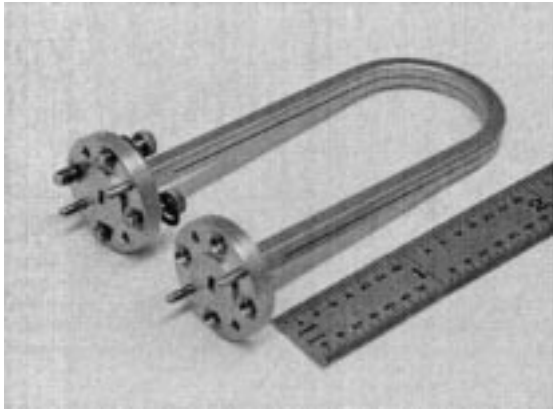


Fig. 3. Prototype phase shifter (scale in inches).

deviation of the U-shaped phase shifter as a function of Δa , and guide dimensions

$$\begin{aligned} \Delta\phi &= \frac{2\pi^2}{\beta a^3} \left(\int_{x=0}^d \delta a(x) dx + R \int_{\theta=0}^{\pi/2} \delta a(d + R \sin \theta) d\theta \right) \\ &= \frac{\pi^2 \Delta a}{\beta a^3 L^3} \left(\frac{3}{4} d^4 + (1 + \pi) R d^3 + \left(\frac{3\pi}{2} + 3 \right) R^2 d^2 \dots \right. \\ &\quad \left. + 6R^3 d + \left(\frac{3\pi}{4} - \frac{2}{3} \right) R^4 \right) \end{aligned} \quad (5)$$

where $L = d + R$, with $R = 0.5$ in and $d = 1.76$ in. The total phase length through the arm is calculated by integrating the wavenumber over the length of the arm and adding the perturbation $\Delta\phi$ from (5).

Meanwhile, as for mechanical considerations, the necessary force required for the deflection Δa is

$$F = -\frac{3EI_y}{L^3} \Delta a \quad (6)$$

where $E \approx 1.17 \times 10^{11}$ N/m² is Young's modulus for oxygen-free electronic grade (OFE) copper (Cu), and the moment of inertia of the cross section is $I_y \approx (AB^3 - ab^3)/12$. With this, one may show that the maximum stress on the copper is

$$\sigma_{\max} = -\frac{3EB}{4L^2} \Delta a. \quad (7)$$

To prevent plastic deformation of the waveguide and, hence, maintain repeatability, we avoid stressing the guide more than 5% of its yield strength $Y \approx 6.9 \times 10^7$ N/m².

With these design scalings in hand, we fashioned a phase shifter using an 8-in length of extruded OFE copper, with interior dimensions as for WR10. A slit was cut through the broad wall by electrodischarge machining (EDM) to facilitate squeezing, and 304L stainless-steel flanges were furnace brazed using CuAu 90/10 alloy. The finished assembly seen in Fig. 3 was then chemically cleaned, as this has been found in waveguide studies to remove any zinc or other unwanted material from redeposit during the EDM process and substantially reduce attenuation.

We characterized the S -matrix for this device under low power using a W -band vector network analyzer (VNA). We took VNA measurements for a series of values of Δa with the help of a stack of feeler gauges used to control the slit gap. The data are summarized in Fig. 4

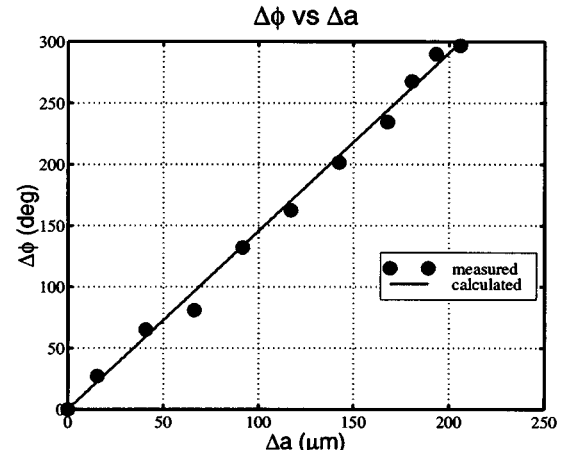


Fig. 4. Measured points overlaid with analytical calculation.

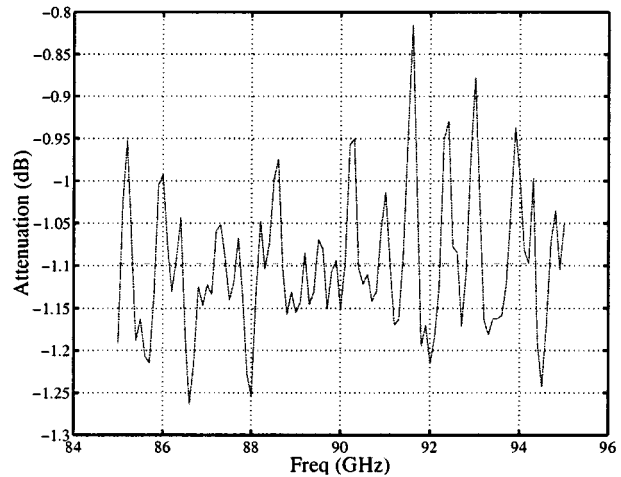


Fig. 5. Attenuation through the phase shifter/recirculator versus frequency. The average attenuation is -1.1 dB.

showing the phase shift versus Δa at 91.4 GHz. The calculated phase shift from (5) is plotted with the measured data in Fig. 4, giving good agreement. The insertion loss seen in Fig. 5 is a factor of 2.7 worse than the theoretical result for straight TE_{10} -mode attenuation in OFE WR10, given by

$$\alpha = \frac{R_s}{Z_0} \left[\frac{\omega^2}{c^2} \frac{1}{b} + \frac{2\pi^2}{a^3} \right] \frac{c}{\omega} \frac{1}{\beta} \quad (8)$$

where $R_s = 0.073 \Omega$ at the operating frequency of 91.4 GHz and $Z_0 = 377 \Omega$ is the impedance of free space. In fact, our experience with straight WR10 of the same material would correspond to 0.15 dB/in or 0.7 dB for this length. In addition, the slit permits radiative loss and TEM-mode coupling.

We tested this device in a traveling-wave resonator circuit, as shown in Fig. 1(b), at power levels above 180 kW, giving field levels above 10.5 MV/m for 100 ns for several million pulses at 10 Hz with no sign of breakdown. Table I shows the field levels for different power levels in WR10 and WR90 waveguide to illustrate the power required for testing under high fields at W -band compared with X -band. Tests at X -band producing equivalent fields would require 2 MW of power.

TABLE I
FIELD LEVELS IN WR10 AND WR90

E(MV/m)	P(W) - WR10
0.8	1.00E+03
2.5	1.00E+04
7.8	1.00E+05
24.7	1.00E+06

E(MV/m)	P(W) - WR90
0.9	1.00E+05
2.8	1.00E+06
8.9	1.00E+07
28.1	1.00E+08

ACKNOWLEDGMENT

The authors would like to thank O. Millican, Stanford Linear Accelerator Center (SLAC), Stanford, CA, and D. Shelly, SLAC, for their expert assistance in fabrication of the phase shifter.

REFERENCES

- [1] C. Adolpshen *et al.*, "RF processing of X -band accelerator structures at the NLCTA," in *Proc. 20th Int. Linac Conf.*, Monterey, CA, Aug. 2000, SLAC-PUB-8573, pp. 21–25.
- [2] D. H. Whittum, "Ultimate gradient in solid-state accelerators," in *Proc. Advanced Accelerator Concepts Workshop*, 1999, pp. 72–85.
- [3] M. E. Hill *et al.*, "Beam-cavity interaction circuit at W -band," *IEEE Trans. Microwave Theory Tech.*, vol. 49, pp. 998–1000, May 2001.
- [4] R. E. Green, Ed., *Machinery's Handbook*. New York: Ind. Press, 1996, p. 239.

An Inverse Scattering Technique for Microwave Imaging of Binary Objects

Ioannis T. Rekanos and Theodoros D. Tsiboukis

Abstract—In this paper, an inverse scattering method for detecting the location and estimating the shape of two-dimensional homogeneous scatterers is presented. It is assumed that the permittivity and conductivity of the scatterer are given. Thus, the method concentrates on reconstructing the domain occupied by the scatterer. The inversion is based on scattered electric far-field measurements and is carried out by a combined finite-element–nonlinear optimization technique. The computational burden is reduced by use of the adjoint-state-vector methodology. Finally, the proposed method is applied to both penetrable and impenetrable scatterers.

Index Terms—Finite-element methods, gradient methods, image reconstruction, inverse scattering, microwave imaging.

I. INTRODUCTION

In most cases concerning electromagnetic inverse scattering, the objective is to reconstruct the distribution of the constitutive parameters

Manuscript received August 19, 1999; revised October 18, 2000.

I. T. Rekanos was with the Division of Telecommunications, Department of Electrical and Computer Engineering, Aristotle University of Thessaloniki, Thessaloniki 54004, Greece. He is now with the Radio Laboratory, Helsinki University of Technology, Espoo, FIN 02015 HUT, Finland (e-mail: rekanos@cc.hut.fi).

T. D. Tsiboukis is with the Division of Telecommunications, Department of Electrical and Computer Engineering, Aristotle University of Thessaloniki, Thessaloniki 54006, Greece (e-mail: tsibukis@vergina.eng.auth.gr).

Publisher Item Identifier S 0018-9480(02)04043-7.

of a specimen using scattered-field measurements. A specific type of this problem consists in estimating the location and shape of a scatterer that has known electromagnetic properties [1]–[3]. In this case, we deal with a binary object reconstruction problem and our aim is to identify the presence or the absence of the scatterer at specified subsections of the domain under investigation. This approach is a very useful tool for nondestructive testing applications [1] and is appropriate for applications where physical limitations do not allow explicit and quantitative reconstruction [2], [3].

The purpose of this paper is to extend the inverse scattering method proposed in [4] to the case of binary objects. As in its initial form, the method combines the finite-element method (FEM) [5] and the Polak–Ribiére nonlinear-conjugate-gradient (NCG) optimization algorithm [6]. Its objective is to minimize an error function that represents the difference between the estimated and measured scattered electric far field. The parameters that describe the scatterer are Boolean variables since they refer to its presence or absence. Hence, the error function has to be modified to a differentiable form in order to compute its gradient. After an appropriate modification [1], the gradient is computed by an FEM-based sensitivity-analysis scheme [7], which is enhanced by the adjoint-state-vector methodology (ASVM) [6]. In numerical results, the proposed method is applied to the reconstruction of penetrable and impenetrable scatterers, while the case of noisy measurements is also examined.

II. DIRECT PROBLEM

We consider an infinitely long, isotropic, and nonmagnetic cylindrical scatterer of bounded cross-section S , which is uniform along the z -axis. It is assumed that the scatterer has constant and known permittivity ϵ_s and conductivity σ_s and is embedded in a homogeneous medium (ϵ_b , σ_b). For a given excitation frequency ω , the scatterer is represented by the complex permittivity contrast (CPC) given by

$$\chi(x, y) = \left[\left(\epsilon_s - j \frac{\sigma_s}{\omega} \right) / \left(\epsilon_b - j \frac{\sigma_b}{\omega} \right) - 1 \right] u(x, y) = \chi_s u(x, y). \quad (1)$$

The function $u(x, y)$ is called *function of support*, and is equal to one or zero when the point (x, y) lies inside or outside S , respectively. If the scatterer is illuminated by a TM-polarized incident wave, then the scattered electric field satisfies the scalar Helmholtz equation. As in [4], we compute the field by applying the FEM, which results in the sparse system of equations

$$\mathbf{S}(\mathbf{u})\mathbf{E} = \mathbf{b}(\mathbf{u}, \mathbf{E}^{\text{inc}}) \quad (2)$$

where the vectors \mathbf{E} and \mathbf{E}^{inc} represent the scattered and incident field values at the nodes of the mesh. Both matrices \mathbf{S} and \mathbf{b} depend on the binary vector $\mathbf{u} = [u_1 \ u_2 \ \dots \ u_M]^T$, where u_m is the constant value of $u(x, y)$ inside the m th element, and M is the total number of elements. After the solution of (2), we calculate the scattered far field by applying the Helmholtz–Kirchhoff integral theorem. In particular, the calculation of the far field at K positions can be represented by the matrix form

$$\mathbf{E}^f = \left[E_1^f \ E_2^f \ \dots \ E_K^f \right]^T = \mathbf{Q}\mathbf{E} \quad (3)$$

where \mathbf{Q} is a sparse matrix associated with the Green's function and its derivative.